Enhanced Deep Learning Approach Based on the Deep Convolutional Encoder–Decoder Architecture for Electromagnetic Inverse Scattering Problems

He Ming Yao, *Student Member, IEEE*, Lijun Jiang, *Fellow, IEEE*, and Wei E. I. Sha, *Senior Member, IEEE*

***Abstract*—This letter proposes a novel deep learning (DL) approach to resolve the electromagnetic inverse scattering (EMIS) problems. The conventional approaches of resolving EMIS problems encounter assorted difficulties, such as high contrast, high computational cost, inevitable intrinsic nonlinearity, and strong ill-posedness. To surmount these difficulties, a novel DL approach is proposed based on a novel complex-valued deep fully convolutional neural network structure. The proposed complex-valued deep learning model for solving EMIS problems composes of an encoder network and its corresponding decoder network, followed by a final pixel-wise regression layer. The complex-valued encoder network extracts feature fragments from received scattered field data, while the role of the complex-valued decoder network is mapping the feature fragments to retrieve the final contrasts (permittivities) of dielectric scatterers. Hence, the proposed deep learning model functions as an "heterogeneous" transformation process, where measured scattering field data is converted into the corresponding contrasts of scatterers. As a consequence, the EMIS problem could be resolved accurately even for extremely high-contrast targets. Numerical benchmarks have illustrated the feasibility and accuracy of our proposed approach. The proposed approach opens a novel path for the deep learning-based real-time quantitative microwave imaging for high-contrast scatterers.**

***Index Terms*—Convolutional neural network, deep learning (DL), electromagnetic inverse scattering (EMIS), high-contrast scatterer.**

I. Introduction

THE electromagnetic inverse scattering (EMIS) has been referred to as the most effective tool for microwave imaging [1], [2]. Its objective is to obtain image of the scatterers from the measured scattering field information [1]–[3]. Thus, solving EMIS problem only requires the received field data outside the target medium. Because of its noncontact and nondestructive characteristics for detection, EMIS has been extensively employed in medical imaging and civil measurement [4]–[6]. Since the last few decades, a lot of modeling approaches have been proposed to resolve the EMIS problem, including Born iterative method (BIM) [7], contrast source inversion [8], [9], contrast-source extend Born [10], and subspace optimization method [11]. Unfortunately, nearly all conventional modeling methods for solving EMIS problem are limited by the avoidable ill-posedness [1]–[3]. High-contrast scatterers also challenge the application of these conventional methods due to the low precision [1]–[3], [7]–[11]. Besides, the high computational complexity and time resulting from these conventional optimization methods can never fulfill the requirement of realizing the microwave imaging for high-contrast scatterers in real time. Finally, the necessary EM coupled equations for conventional methods cannot be independent on the complex Green's functions, which have to be specifically constructed according to the practical application scenarios [12], [13].

Deep learning (DL) is rapidly developing in every corner of the modern computational science [14], [15]. It is promoting the development of conventional computational electromagnetics. There have been a large number of representative applications, involving scientific computation [16]–[18], remote sensing imaging [19], [20] and hybrid field-circuit simulation [21], [22]. In fact, machine learning has been employed in the EMIS problem. The artificial neural network has been utilized to resolve the EMIS problem in [23], [24]. Unfortunately, these approaches are greatly limited to specific application scenarios, where the methods are only valid for scatterers with a set of specific parameters pattern [23], [24]. Recently, a number of works based on DL techniques have been applied to EM problems [25]–[36], including solving the forward EM problems and the EMIS problems. In [25]–[27], the DL approaches are used to offer relatively better performance. At present, these DL-based methods are partially dependent on the conventional methods and need to use the initial inputs provided by traditional methods to conduct further operation, such as initial inputs from the backpropagation method [37]. Moreover, although some previous works have introduced DL into solving the EMIS problem and obtained better performance than the conventional methods [29], the application of representative two-step cascaded DL method increases the computational complexity of solving the EMIS problem.

In this letter, we propose a novel DL method based on the deep convolutional encoder–decoder structure to resolve EMIS problems. The model is constructed on the complex-valued

Manuscript received September 22, 2019; revised November 20, 2019; accepted December 2, 2019. Date of publication May 18, 2020; date of current version July 7, 2020. This work was supported in part by the Research Grants Council of Hong Kong under Grant GRF 17207114 and Grant GRF 17210815, in part by the Asian Office of Aerospace Research and Development (AOARD) under Grant FA2386-17-1-0010, in part by the National Natural Science Foundation (NSFC) under Grant 61271158, and in part by the Hong Kong University Grants Committee (UGC) under Grant AoE/P04/08. *(Corresponding authors: Lijun Jiang; Wei E. I. Sha.)*

He Ming Yao and Lijun Jiang are with the Department of Electrical and Electronic Engineering, The University of Hong Kong, Hong Kong (e-mail: yaohmhk@connect.hku.hk; jianglj@hku.hk).

Wei E. I. Sha is with the Key Laboratory of Micro-Nano Electronic Devices and Smart Systems of Zhejiang Province, College of Information Science and Electronic Engineering, Zhejiang University, Hangzhou 310027, China (e-mail: weisha@zju.edu.cn).

Digital Object Identifier 10.1109/LAWP.2020.2995455

1536-1225 © 2020 IEEE. Personal use is permitted, but republication/redistribution requires IEEE permission.
See https://www.ieee.org/publications/rights/index.html for more information.

Authorized licensed use limited to: Zhejiang University. Downloaded on July 26,2020 at 06:31:34 UTC from IEEE Xplore. Restrictions apply.

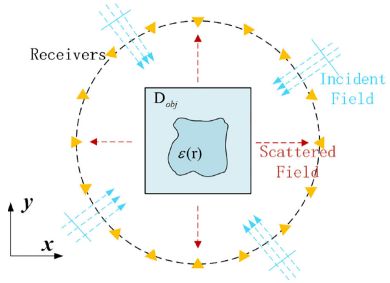

Fig. 1. TM$_z$ wave scattering for the region $D_{\rm obj}$.

deep convolutional neural network (DConvNet), consisting of an encoder network and its corresponding decoder network. It can effectively reconstruct the permittivity (contrast) "images" of dielectric objects from the received scattered field information. The advantages of the proposed approach are as follows.

1) Effectiveness: The new DL approach can effectively work on the high-contrast scatterers, compared to the conventional methods.
2) Simplicity: The DL framework can avoid calculating complicated Green's functions to reduce the high complexity of the traditional approaches.
3) Accuracy: The accuracy of the proposed method is much higher than the conventional methods.

II. Theory and Formulation

A. Problem Formulation

Fig. 1 presents the representative schematic of EMIS, where an object domain $D_{\rm obj}$ is surrounded by M equally spaced receivers. The object dielectric domain $D_{\rm obj}$ is gridded into uniform $N \times N$ fragments and is illuminated by the TM$_z$ incident field $E^{\rm in}$. The scattered field measured by M receivers is denoted as E^s. While this 2-D configuration is employed to illustrate the mechanism of our approach, we emphasize our approach can also be employed to 3-D configuration. To formulate the whole process of the EMIS, two governing equations are introduced in (1) and (2), which are also called Lippmann–Schwinger equations [38].

The first formula for the EMIS mainly formulates the interaction among the field of scatterer pieces in $D_{\rm obj}$, as in

$$E^{\rm in}(\boldsymbol{r}) = E^t(\boldsymbol{r}) - k_0^2 \int_{D_{\rm obj}} G(\boldsymbol{r},\boldsymbol{r}')\,\chi(\boldsymbol{r}')\,E^t(\boldsymbol{r}')\,d\boldsymbol{r}' \quad (1)$$

where $G(\boldsymbol{r},\boldsymbol{r}')$ is denoted as the Green's function and we have $G(\boldsymbol{r},\boldsymbol{r}') = -\frac{j}{4}H_0^{(2)}(k_0|\boldsymbol{r}-\boldsymbol{r}'|)$ for 2-D TM$_z$ wave. $H_0^{(2)}$ is the second kind zeroth order Hankel function while k_0 is the wave number in the free space. $\boldsymbol{r}' = (x', y')$ and $\boldsymbol{r} = (x, y)$ stands for the source and field points in object domain $D_{\rm obj}$, respectively. While E^t stands for the total electronic field, the contrast function can be denoted to be $\chi(\boldsymbol{r}') = \varepsilon_r(\boldsymbol{r}') - 1$.

Based on (1), the scattered field is described as the reradiation by the total field E^t in scatterers, and the relationship between E^s and E^t is shown as follows:

$$E^s(\boldsymbol{r}) = k_0^2 \int_{D_{\rm obj}} G(\boldsymbol{r},\boldsymbol{r}')\,\chi(\boldsymbol{r}')\,E^t(\boldsymbol{r}')\,d\boldsymbol{r}' \quad (2)$$

where $\boldsymbol{r} = (x_R, y_R)$ stands for the coordinate of the receivers, whereas $\boldsymbol{r}' = (x', y')$ is on the source piece in $D_{\rm obj}$.

The final target of the EMIS problem is to retrieve the contrast χ (or permittivity ε_r) of the scatterer by using the scattered field received by M receivers around the $D_{\rm obj}$. Directly solving the coupled (1) and (2) to retrieve the contrast is very hard [1], [3]. Usually, the conventional methods construct an objective function $f(\chi)$, as shown in (3), and attempt to retrieve contrast by optimization methods [3].

$$\min: f(\chi) = \sum_{i=1}^{N_i} \left\| E_i^s - E_i^s(\chi)' \right\|^2 + \alpha T(\chi) \quad (3)$$

where the received scattering field E_i^s is induced by N_i separate incident field $E^{\rm in}$ onto $D_{\rm obj}$, and the optimized scattering fields $E_i^s(\chi)'$ approaches the measured scattered field E_i^s by iterative optimization computation in (3). $\|\cdot\|$ is the Euclidian length, whereas T is denoted as the regularization for balancing data fitting and the solution stability [27], [39].

In the conventional methods, the (1) and (2) are first transformed into the following discretized coupled equations [1], [3] for the optimization process in (3), where the object domain $D_{\rm obj}$ is gridded into uniform pieces, and the contrast and the total electric field of each individual piece are treated as the piecewise constant

$$\bar{E}^s = \overline{\overline{G}}_R \cdot \mathrm{diag}\left(\bar{E}^t\right) \cdot \bar{\chi} \quad (4)$$

$$\bar{E}^{\rm in} = \bar{E}^t - \overline{\overline{G}}_D \cdot \mathrm{diag}\left(\bar{E}^t\right) \cdot \bar{\chi} \quad (5)$$

where the size of the matrices $\overline{\overline{G}}_R$ and $\overline{\overline{G}}_D$ are $M \times N^2$ and $N^2 \times N^2$, respectively. We have $\overline{\overline{G}}_R = k_0^2 S_{n'} G(\boldsymbol{r}_{n_r}, \boldsymbol{r}_{n'})$ and $\overline{\overline{G}}_D = k_0^2 S_{n'} G(\boldsymbol{r}_n, \boldsymbol{r}_{n'})$, where $S_{n'}$ is the area of source piece. We also have $n_r = 1, \ldots, M$, $n = 1, \ldots, N^2$, and $n' = 1, \ldots, N^2$.

Unfortunately, solving (3) by conventional optimization methods also face challenges due to its nonlinearity [1], [3], particularly for high contrast situations [1], [3].

B. Encoder–Decoder Structure for EMIS

To solve the problem of the high-contrast scatterers with high accuracy, a novel DL approach is proposed based on the DConvNet. In the novel approach, the deep convolutional encoder–decoder structure is employed to transform original scattering fields into the contrasts (permitivitties) of scatterers in the objective region. Considering the difficulties of collecting the huge number of training samples by real experiments, the simulation data are applied to train DL models.

The proposed DConvNet is revised based on the structure of SegNet [40] that has been widely employed for the image segmentation. Typical ConvNets [41], [42] comprises of five different kinds of layer unit: input layers, convolutional layers, activation layers, pooling layers, and fully connected layers. The typical ConvNet arthitecture is constructed based on these layer unit. In this work, these typical layers are stacked together to design the proposed DConvNet to solve the EMIS problem.

The specific internal structure of our DConvNet is presented in Fig. 2. Its input is the scattering field E^s, referred to as "field data," which is the matrix with the size of the $M \times N_i \times 2$. M represents M receivers and N_i is the total number of the incident

Authorized licensed use limited to: Zhejiang University. Downloaded on July 26,2020 at 06:31:34 UTC from IEEE Xplore. Restrictions apply.

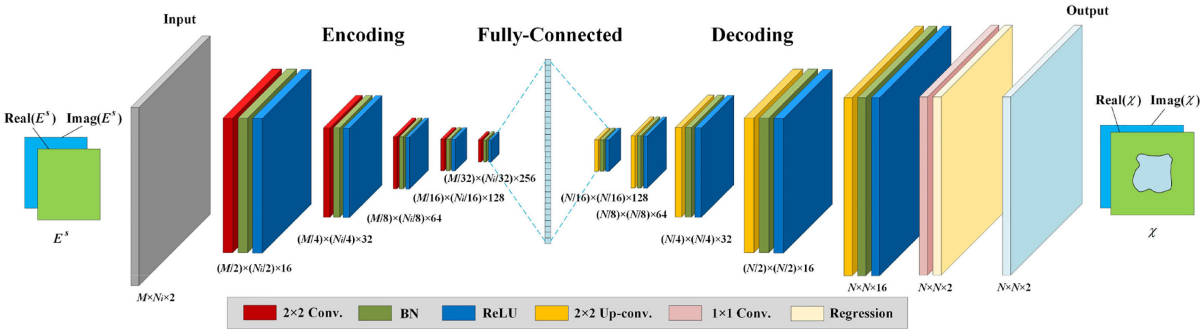

Fig. 2. DConvNet architecture. Conv. is convolution, BN is batch normalization, ReLU is rectified linear unit, whereas Up-conv. represents up-convolution.

field, whereas the real and imaginary parts of E^s stand for its two tubes, which is presented in Fig. 2. Meanwhile, its output is a $N \times N \times 2$ matrix comprising of the real and imaginary parts of the target permittivity.

In the DConvNet, the designed convolutional and activation layers in encoding part act to capture features of input. The parameters, including the convolutional layer number, the filter (kernel) number and its size, etc., are also shown in Fig. 2 [41], [42]. Then, the decoding part feeds into a final regression layer, which finally provides the prediction of the contrast χ. This prediction is denoted as the final output of the DConvNet. The loss function is the so-called half-mean-squared error between these predicted responses of each pixel and the true label, as in (6).

$$\text{loss} = \frac{1}{2}\sum_{p=1}^{HWC}(t_p - y_p)^2 \tag{6}$$

where *H*, *W*, and *C* are set as the height, width, and channel number of the final output. *p* indexes into each pixel of the target *t* and the prediction *y*.

In Fig. 2, the designed DConvNet mainly involves three parts: encoding, decoding, and fully connected. The first part encodes "field data" E^s layer by layer and refines it into chunks of information fragments, whereas the corresponding decoding part reorganizes the extracted information fragments layer by layer until the final scatterer contrast χ is generated. The middle fully connected intermediate part can be seen as the bridge linking the encoding and decoding parts. In detail, the encoding part consists of repeated applications of 2×2 convolution with its stride equal to 2, rectified linear unit (ReLU) and batch normalization (BN). Comparatively, the corresponding decoding part composes of the repeated applications of 2×2 up-convolution with its stride equal to 2, BN and ReLU operations, whereas a 1×1 convolution layer and the regression layer are set at the end of this part, as presented in Fig. 2. The selection of parameters and the detailed operation in those layers can refer to [25]–[27], [29], [41]–[44]. Generally, 2×2 filter in convolutional layers can decrease the parameter number on filter, while the stride 2 can increase or decrease the size of the middle layers for encoding and decoding parts [29], [40], [44]. The nonlinear relation between input and output is denoted as the following formula, while Γ is denoted as the nonlinear operation of the proposed DL model:

$$\chi = \Gamma\left(E^s\right). \tag{7}$$

The entire process is summarized as a "heterogeneous" process. It transforms received scattering field into the final contrast of the target scatterers. In the process, the complex-valued DConvNet directly uses E^s as the input, while the output is chosen as χ. Hence, the proposed complex-valued DConvNet entirely replaces the conventional methods and complete all their operations, i.e., the initial contrast selection and the later operation processes [7]–[11]. Besides, we highlight that the whole process of constructing model is independent on the calculation of Green's function, and it can reduce the ill-possdness of the conventional methods [7]–[11], thanks to its the data-driven characteristics, which are based on the training to obtain more prior knowledge [29], [30]. Moreover, we emphasize that the proposed DConvNet can completely finish the reconstruction operation by one model, which is simpler than the two-step approach [29]. Finally, unlike [27], [29], [43], [44], the proposed DConvNet directly finishes the "heterogeneous" transformation from scattering field to contrast by encoder–decoder structure and does not need the skip connection in the U-Net to realize the residual learning.

The newly proposed DConvNet model is implemented into MATLAB 2019a with the DL Toolbox [45]. Adaptive moment estimation (Adam) optimizer is used for optimizing the above-mentioned loss function. Compared with other optimizers, including stochastic gradient descent, Adam optimizer generally navigates through the loss surface more favourably [46], [47].

There are several issues about the above-mentioned proposed model that need to be emphasized.

1) *Fully connected intermediate layer:* Unlike the conventional encoder–decoder structure in SegNet [40], fully connected intermediate layer is added between the encoding part and decoding part in our DConvNet. By the operation of the fully connected intermediate layer, the information fragments extracted from encoding part are reorganized into the new feature maps and are further transformed into the final output. The added fully connected intermediate layer effectively increases the capacity of converting "heterogeneous" features from field into contrast.
2) *Complex-valued input and output:* As a representative complex-valued problem, both the received electronic field and the contrast of the object domain are complex valued for the EMIS problem. Thus, the original channel number of both input and output of the SegNet has to be revised [40], so that their real and imaginary parts could be adapted in the different channels. Hence, the novel model can be more adaptable and flexible for reconstructing contrast in real situations.

Authorized licensed use limited to: Zhejiang University. Downloaded on July 26,2020 at 06:31:34 UTC from IEEE Xplore. Restrictions apply.

3) *Computational complexity:* For the proposed DConvNet, the computation mainly depends on the repeative application of convolutions, BN and ReLU, where the filter kernel is tiny in the DConvNet and its operation count is mainly dominated by convolution operation [27], [43]. For the encoder part, the network has the input with the size of $M \times N_i \times 2$, R filters with the size of $K \times K$ each layer and f layers. Thus, its computation complexity of the DConvNet is $O(MN_iK^2R^2f)$ [44], [48]. Moreover, the computation of the decoding part can be treated as the same operation of encoding part but from the opposite direction. Thus, with all similar hyperparameters, including filter number and size, etc., only the size of output (equivalent to the input of encoding part) is replaced by $N \times N \times 2$. Thus, the computational complexity of decoding part is $O(N^2K^2R^2f)$. Generally, we tend to choose the size of input field "image" to be approximated to the size of output contrast "image", which has also been done in [27], [29], [44]. Hence, the computational complexity of the entire network can be approximated to $O(N^2K^2R^2f)$ [44], [48]. Besides, its storage mainly depends on the size of the filters and biases. Thus, the storage of our DConvNet is $O(K^2R^2f)$ [44], [48].

III. Numerical Examples

To validate the precision and effectiveness of the newly proposed DL approach, we use the popular MNIST dataset as the target scatterers samples [25]–[27]. The size of each sample in MNIST dataset is set to about 2.25 $\lambda \times 2.25\ \lambda$ (the wavelength $\lambda = 1$ m in free space) and is gridded into 32×32 uniform pieces (i.e., $N = 32$). While 32 receivers ($M = 32$) are uniformly set around D_{obj} with the distance 30 λ, the TM_z incident plane waves come from 32 different directions to impinge on the object domain D_{obj} with the incident angles uniformly distributed within [0°, 360°), (i.e. $N_i = 32$). In this section, the full-wave EM simulations [49] are employed for all samples to create both training and testing dataset. More details about the similar numerical setup can refer to [25]–[29], [43], [44]. By using the MNIST dataset, the digit-shaped scatterers are given the extremely high relative permittivity $\varepsilon_r = 8$, which is the much challengable task for the conventional methods. A total of 8000 samples in MNIST dataset are randomly chosen to train the proposed DL model, whereas another 1000 samples are employed for testing. Two quantitative indicators, i.e., normalized mean-square error (NMSE) and structural similarity index (SSIM), are employed to evaluate the result of retrieved "images", as what has been done in [25]–[27]. Moreover, the BIM is applied to retrieve the permittivities of the testing samples for comparison. The results are shown in Fig. 3.

Fig. 3 demonstrates the comparisons among the ground truths, reconstructed images of BIM, and the reconstructed results of the DConvNet approach. Evidently, the final reconstruction outputs of the proposed method have good agreements with the ground truth. However, for these high-contrast cases, the BIM never offers any acceptable result.

In Fig. 4, the statistical analyses for the testing results are presented: the NMSE average of reconstructed results obtained by the DConvNet is around 0.08, and the SSIM average obtained from the proposed approach can reach around 0.8. Therefore, the newly proposed DL method can resolve the EMIS problem with excellent performances.

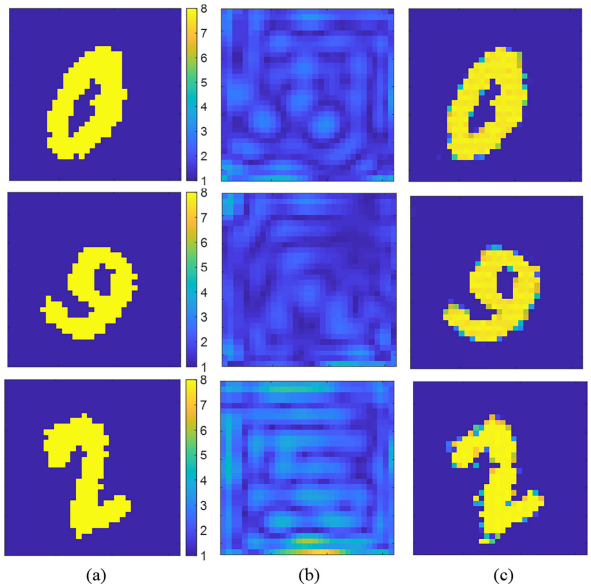

Fig. 3. Comparisons of reconstructed relative permittivities of digit-shaped scatterers. (a) Ground truth. (b) Reconstructed relative permittivities of the BIM. (c) Reconstructed relative permittivities of the proposed DConvNet. (The third row presents the relative bad reconstruction results.)

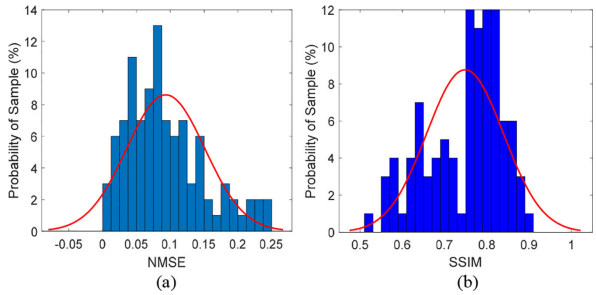

Fig. 4. Statistical histograms of the image quality for the reconstructed permittivities and fitting of its normal density function. (a) NMSE results from the DConvNet method. (b) SSIM results from the DConvNet method.

IV. Conclusion

A novel DL approach based on the complex-valued DConvNet structure is proposed to resolve the EMIS problems. The traditional methods are challenged by various difficulties, including high-contrast case and the ill-posedness. The proposed complex-valued DL model comprises of a complex-valued convolutional encoder–decoder architecture. The encoder network extracts feature fragments from measured scattering field data, whereas decoder network then reorganizes the feature fragments to retrieve the final reconstructed contrasts of scatterers. As a result, the EMIS problems can be resolved with high precision even for extremely high-contrast scatterers. Numerical benchmarks illustrate the validity of this DL approach. The proposed DL method for the EMIS problem offers a novel tool to realize the quantitative microwave imaging in real time.

Authorized licensed use limited to: Zhejiang University. Downloaded on July 26,2020 at 06:31:34 UTC from IEEE Xplore. Restrictions apply.

REFERENCES

[1] M. Pastorino, *Microwave Imaging*. New York, NY, USA: Wiley, 2010.

[2] P. M. Meaney *et al.*, "A clinical prototype for active microwave imaging of the breast," *IEEE Trans Microw. Theory Techn.*, vol. 48, no. 11, pp. 1841–1853, Nov. 2000.

[3] M. Li *et al.*, "Electromagnetic inverse problems [Guest Editorial]," *IEEE Antennas Propag. Mag.*, vol. 59, no. 5, pp. 9–115, Oct. 2017.

[4] W. C. Chew *et al.*, "Nonlinear diffraction tomography: The use of inverse scattering for imaging," *Int. J. Imag. Syst. Technol.*, vol. 7, pp. 16–24, 1996.

[5] A. Abubakar *et al.*, "Application of the multiplicative regularized Gauss–Newton algorithm for three-dimensional microwave imaging," *IEEE Trans. Antennas Propag.*, vol. 60, no. 5, pp. 2431–2441, May 2012.

[6] J. Behura, K. Wapenaar, and R. Snieder, "Autofocus imaging: Image reconstruction based on inverse scattering theory," *Geophysics*, vol. 79, no. 3, pp. A19–A26, 2014.

[7] M. Moghaddam and W. C. Chew, "Study of some practical issues in inversion with the Born iterative method using time-domain data," *IEEE Trans. Antennas Propag.*, vol. 41, no. 2, pp. 177–184, Feb. 1993.

[8] A. Abubakar *et al.*, "The contrast source inversion method for location and shape reconstructions," *Inverse Problems*, vol. 18, no. 2, pp. 495–510, 2002.

[9] M. Li, O. Semerci, and A. Abubakar, "A contrast source inversion method in the wavelet domain," *Inverse Problems*., vol. 29, no. 025015, pp. 1–19, 2013.

[10] L. Crocco, M. D'Urso, and T. Isernia, "Testing the contrast source extended Born inversion method against real data: The TM case," *Inverse Problems*, vol. 21, 2005, Art. no. S33.

[11] X. Ye, Y. Zhong, and X. Chen, "Reconstructing perfectly electric conductors by the subspace-based optimization method with continuous variables," *Inverse Problems*, vol. 27, no. 5, May 2011, Art. no. 055011.

[12] G. Boudarham *et al.*, "Spectral imaging of individual split-ring resonators," *Phys. Rev. Lett.*, vol. 1, no. 5, 2010, Art. no. 255501.

[13] R. Wang, B. Z. Wang, Z. S. Gong, X. Ding, "Far-field subwavelength imaging with near-field resonant metalens scanning at microwave frequencies," *Sci. Rep.*, vol. 5, Jun. 2015, Art. no. 11131.

[14] Y. LeCun, Y. Bengio, and G. Hinton, "Deep learning," *Nature*, vol. 521, no. 7553, pp. 436–444, 2015.

[15] C. M. Bishop, *Pattern Recognition and Machine Learning*. Berlin, Germany: Springer, Aug. 2006.

[16] H. M. Yao, L. J. Jiang, and Y. W. Qin, "Machine learning based method of moments (ML-MoM)," in *Proc. IEEE Int. Symp. Antennas Propag. USNC/URSI Nat. Radio Sci. Meeting*, San Diego, CA, 2017, pp. 973–974, doi: 10.1109/APUSNCURSINRSM.2017.8072529.

[17] W. Tang *et al.*, "Study on a Poisson's equation solver based on deep learning technique," in *Proc. IEEE Elect. Design Adv. Packag. Syst. Symp. (EDAPS)*, 2017, pp. 1–3, doi: 10.1109/EDAPS.2017.8277017.

[18] H. M. Yao and L. Jiang, "Machine-learning-based PML for the FDTD method," *IEEE Antennas Wireless Propag. Lett.*, vol. 18, no. 1, pp. 192–196, Jan. 2019.

[19] L. Zhao, J. K. feng, K. Miao, X. G. Leng, and H. X. Zou, "Deep convolutional highway unit network for SAR target classification with limited labeled training data," *IEEE Geosci. Remote Sens. Lett.*, vol. 14, no. 7, pp. 1091–1095, Jul. 2017.

[20] S. Z. Chen, H. P. Wang, F. Xu, and Y. Q. Jin, "Target classification using the deep convolutional networks for SAR images," *IEEE Trans. Geosci. Remote Sens.*, vol. 54, no. 8, pp. 4806–4817, Aug. 2016.

[21] H. H. Zhang, L. J. Jiang, and H. M. Yao, "Embedding the behavior macromodel into TDIE for transient field-circuit simulations," *IEEE Trans. Antennas Propag.*, vol. 64, no. 7, pp. 3233–3238, Jul. 2016.

[22] H. H. Zhang, L. J. Jiang, H. M. Yao, and Y. Zhang, "Transient heterogeneous electromagnetic simulation with DGTD and behavioral macromodel," *IEEE Trans. Electromagn. Compat.*, vol. 59, no. 4, pp. 1152–1160, Aug. 2017.

[23] S. Caorsi and P. Gamba, "Electromagnetic detection of dielectric cylinders by a neural network approach," *IEEE Trans. Geosci. Remote Sens.*, vol. 37, no. 2, pp. 820–827, Mar. 1999.

[24] I. T. Rekanos, "Inverse scattering of dielectric cylinders by using radial basis function neural networks," *Radio Sci.*, vol. 36, no. 5, pp. 841–849, 2001.

[25] L. Li, L. G. Wang, and F. L. Teixeira, "Performance analysis and dynamic evolution of deep convolutional neural network for electromagnetic inverse scattering," *IEEE Antennas Wireless Propag. Lett.*, vol. 18, no. 11, pp. 2259–2263, Nov. 2019, doi: 10.1109/LAWP.2019.2927543.

[26] L. Li *et al.*, "DeepNIS: Deep neural network for nonlinear electromagnetic inverse scattering," *IEEE Trans. Antennas and Propag.*, vol. 67, no. 3, pp. 1819–1825, Mar. 2019.

[27] Z. Wei and X. Chen, "Deep-learning schemes for full-wave nonlinear inverse scattering problems," *IEEE Trans. Geosci. Remote Sens.*, vol. 57, no. 4, pp. 1849–1860, Apr. 2019.

[28] H. M. Yao, M. Li, and L. Jiang, "Applying deep learning approach to the far-field subwavelength imaging based on near-field resonant metalens at microwave frequencies," *IEEE Access*, vol. 7, pp. 63801–63808, 2019.

[29] H. M. Yao, W. E. I. Sha, and L. Jiang, "Two-step enhanced deep learning approach for electromagnetic inverse scattering problems," *IEEE Antennas Wireless Propag. Lett.*, vol. 18, no. 11, pp. 2254–2258, Jul. 2019.

[30] R. Guo *et al.*, "Supervised descent learning technique for 2-D microwave imaging," *IEEE Trans. Antennas Propag.*, vol. 67, no. 5, pp. 3550–3554, May 2019.

[31] Y. Sun *et al.*, "Efficient and accurate inversion of multiple scattering with deep learning," *Opt. Express*, vol. 26, no. 11, pp. 14678–14688, Apr. 2018.

[32] H. M. Yao, W. E. I. Sha, and L. J. Jiang, "Applying convolutional neural networks for the source reconstruction," *Prog. Electromagn. Res. M*, vol. 76, pp. 91–99, 2018.

[33] J. Adler *et al.*, "Solving ill-posed inverse problems using iterative deep neural networks," *Inverse Problems*, vol. 33, no. 12, pp. 1–24, Nov. 2017.

[34] S. J. Hamilton and A. Hauptmann, "Deep D-Bar: Real-time electrical impedance tomography imaging with deep neural networks," *IEEE Trans. Med. Imag.*, vol. 37, no. 10, pp. 2367–2377, Oct. 2018.

[35] H. M. Yao and L. J. Jiang, "Machine learning based neural network solving methods for the FDTD method," in *Proc. IEEE Int. Symp. Antennas Propag. USNC/URSI Nat. Radio Sci. Meeting*, Boston, MA, USA, 2018, pp. 2321–2322.

[36] H. M. Yao and L. Jiang, "Enhanced PML based on the long short term memory network for the FDTD method," *IEEE Access*, vol. 8, pp. 21028–21035, 2020.

[37] K. Belkebir, P. C. Chaumet, and A. Sentenac, "Superresolution in total internal reflection tomography," *J. Opt. Soc. Amer. A, Opt. Image Sci.*, vol. 22, no. 9, pp. 1889–1897, 2005.

[38] M. A. Fiddy and R. S. Ritter, *Introduction to Imaging from Scattered Fields*. Boca Raton, FL, USA: CRC Press, 2014.

[39] A. L. da Cunha, J. Zhou, and M. N. Do, "The nonsubsampled contourlet transform: Theory, design, and applications," *IEEE Trans. Image Process.*, vol. 15, no. 10, pp. 3089–3101, Oct. 2006.

[40] V. Badrinarayanan, A. Kendall, and R. Cipolla, "SegNet: A deep convolutional encoder–decoder architecture for image segmentation," *IEEE Trans. Pattern Anal. Mach. Intell.*, vol. 39, no. 12, pp. 2481–2495, Dec. 2017.

[41] A. Krizhevsky, I. Sutskever, and G. Hinton, "ImageNet classification with deep convolutional neural networks," *Commun. ACM*, vol. 60, no. 6, pp. 84–90, 2017.

[42] Y. Zhang, D. Zhao, J. Sun, G. Zou, and W. Li, "Adaptive convolutional neural network and its application in face recognition," *Neural Process. Lett.*, vol. 43, no. 2, pp. 389–399, 2015.

[43] O. Ronneberger, P. Fischer, and T. Brox, "U-net: Convolutional networks for biomedical image segmentation," in *Proc. 18th Int. Conf. Med. Image Comput. Comput. Assisted Intervention*, 2015, pp. 234–241.

[44] K. H. Jin *et al.*, "Deep convolutional neural network for inverse problems in imaging," *IEEE Trans. Image Process.*, vol. 26, no. 9, pp. 4509–4522, Sep. 2017.

[45] P. Kim, *MATLAB Deep Learning*. New York, NY, USA: Apress, 2017.

[46] D. P. Kingma and J. L. Ba, "Adam: A method for stochastic optimization," in *Proc. Int. Conf. Learn. Representation*, 2015, pp. 1–41.

[47] N. S. Keskar *et al.*, "On large-batch training for deep learning: Generalization gap and sharp minima," 2017. [Online]. Available: https://arxiv.org/abs/1609.04836

[48] J. Cong and B. Xiao, "Minimizing computation in convolutional neural networks," in *Proc. Int. Conf. Artif. Neural Netw.*, 2014, pp. 281–290.

[49] M. F. Catedra, R. P. Torres, J. Basterrechea, and E. Gago. *The CG-FFT Method: Application of Signal Processing Techniques to Electromagnetics*. Boston, MA, USA: Artech House, 1995.

Authorized licensed use limited to: Zhejiang University. Downloaded on July 26,2020 at 06:31:34 UTC from IEEE Xplore. Restrictions apply.